nature neuroscience

Supplementary information

https://doi.org/10.1038/s41593-024-01791-4

Astrocyte transcriptomic changes along the spatiotemporal progression of Alzheimer's disease

In the format provided by the authors and unedited

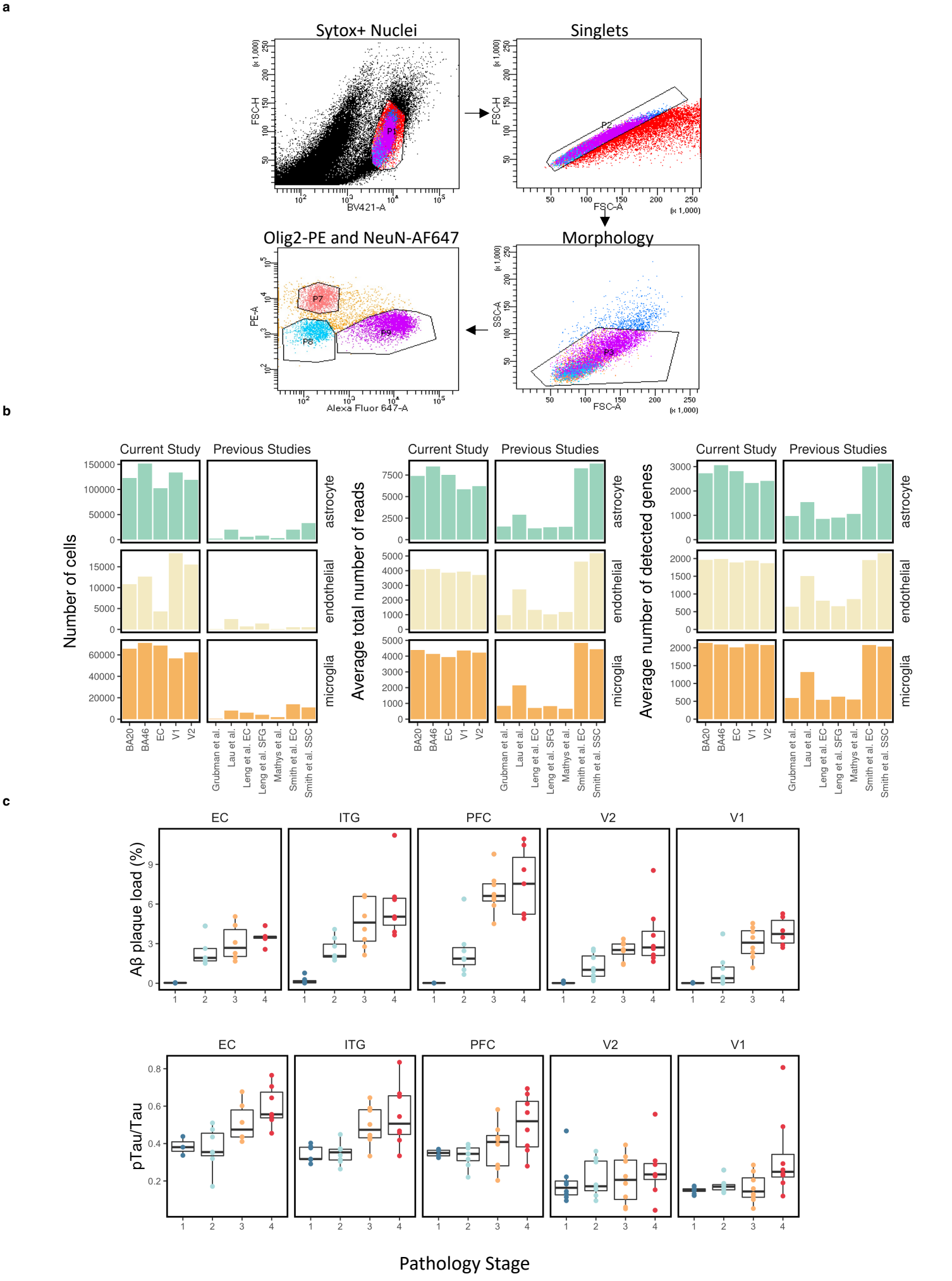
a
Sytox+ Nuclei
Singlets
Olig2-PE and NeuN-AF647
Morphology
FSC-H
BV421-A
FSC-A
PE-A
Alexa Fluor 647-A
SSC-A
P1
P2
P3
P7
P8
P9
b
Current Study
Previous Studies
Number of cells
Average total number of reads
Average number of detected genes
astrocyte
endothelial
microglia
BA20
BA46
EC
V1
V2
Grubman et al.
Lau et al.
Leng et al. EC
Leng et al. SFG
Mathys et al.
Smith et al. EC
Smith et al. SSC
c
EC
ITG
PFC
V2
V1
Aβ plaque load (%)
pTau/Tau
Pathology Stage


AQP4
EC
V1

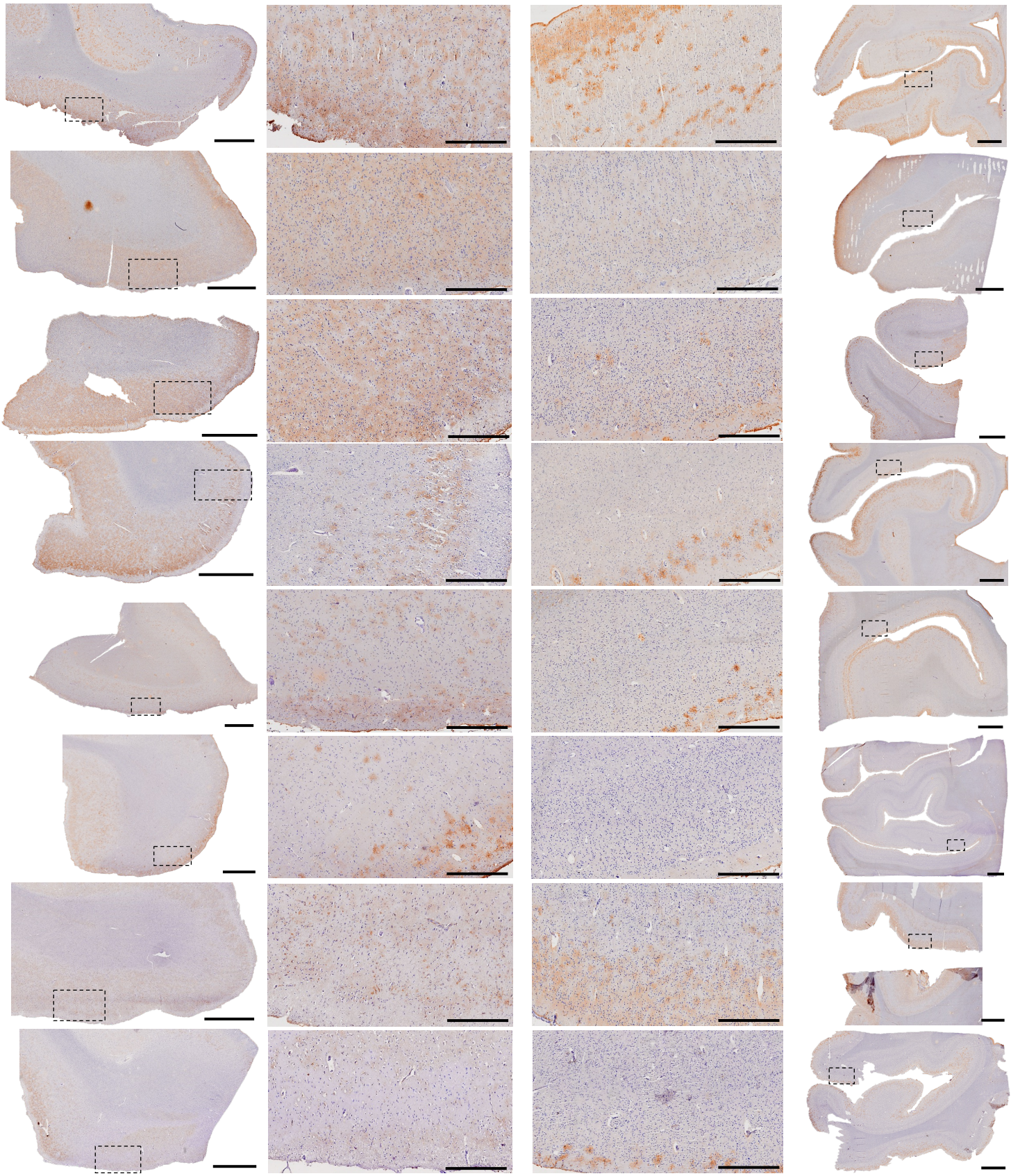
GJA1
EC
V1

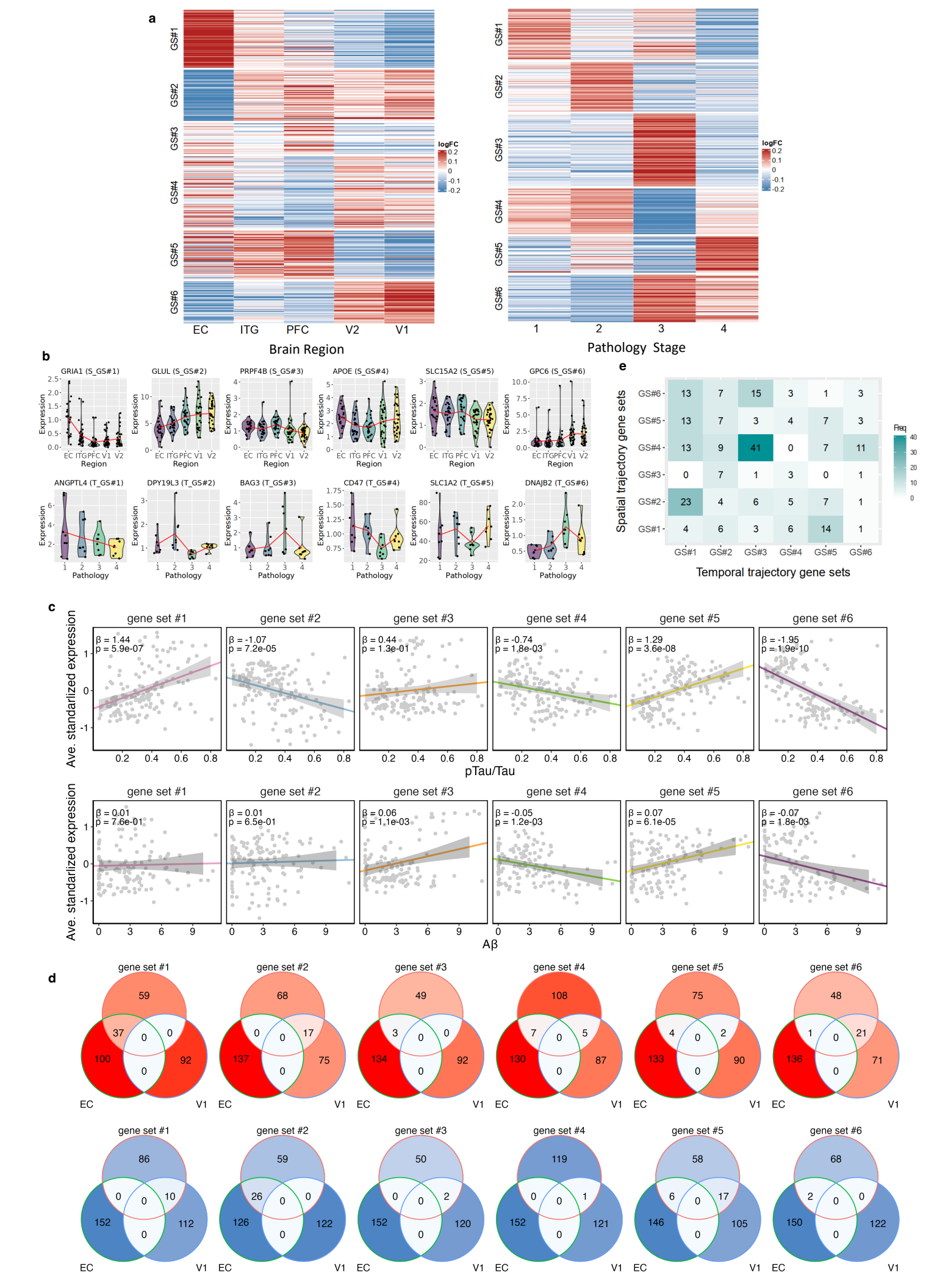
a
GS#1
GS#2
GS#3
GS#4
GS#5
GS#6
logFC
0.2
0.1
0
-0.1
-0.2
EC
ITG
PFC
V2
V1
Brain Region
1
2
3
4
Pathology Stage
b
GRIA1 (S_GS#1)
GLUL (S_GS#2)
PRPF4B (S_GS#3)
APOE (S_GS#4)
SLC15A2 (S_GS#5)
GPC6 (S_GS#6)
ANGPTL4 (T_GS#1)
DPY19L3 (T_GS#2)
BAG3 (T_GS#3)
CD47 (T_GS#4)
SLC1A2 (T_GS#5)
DNAJB2 (T_GS#6)
Expression
Region
Pathology
e
Spatial trajectory gene sets
Temporal trajectory gene sets
Freq
c
gene set #1
gene set #2
gene set #3
gene set #4
gene set #5
gene set #6
β = 1.44
p = 5.9e-07
β = -1.07
p = 7.2e-05
β = 0.44
p = 1.3e-01
β = -0.74
p = 1.8e-03
β = 1.29
p = 3.6e-08
β = -1.95
p = 1.9e-10
Ave. standardized expression
pTau/Tau
β = 0.01
p = 7.6e-01
β = 0.01
p = 6.5e-01
β = 0.06
p = 1.1e-03
β = -0.05
p = 1.2e-03
β = 0.07
p = 6.1e-05
β = -0.07
p = 1.8e-03
Aβ
d
EC
V1

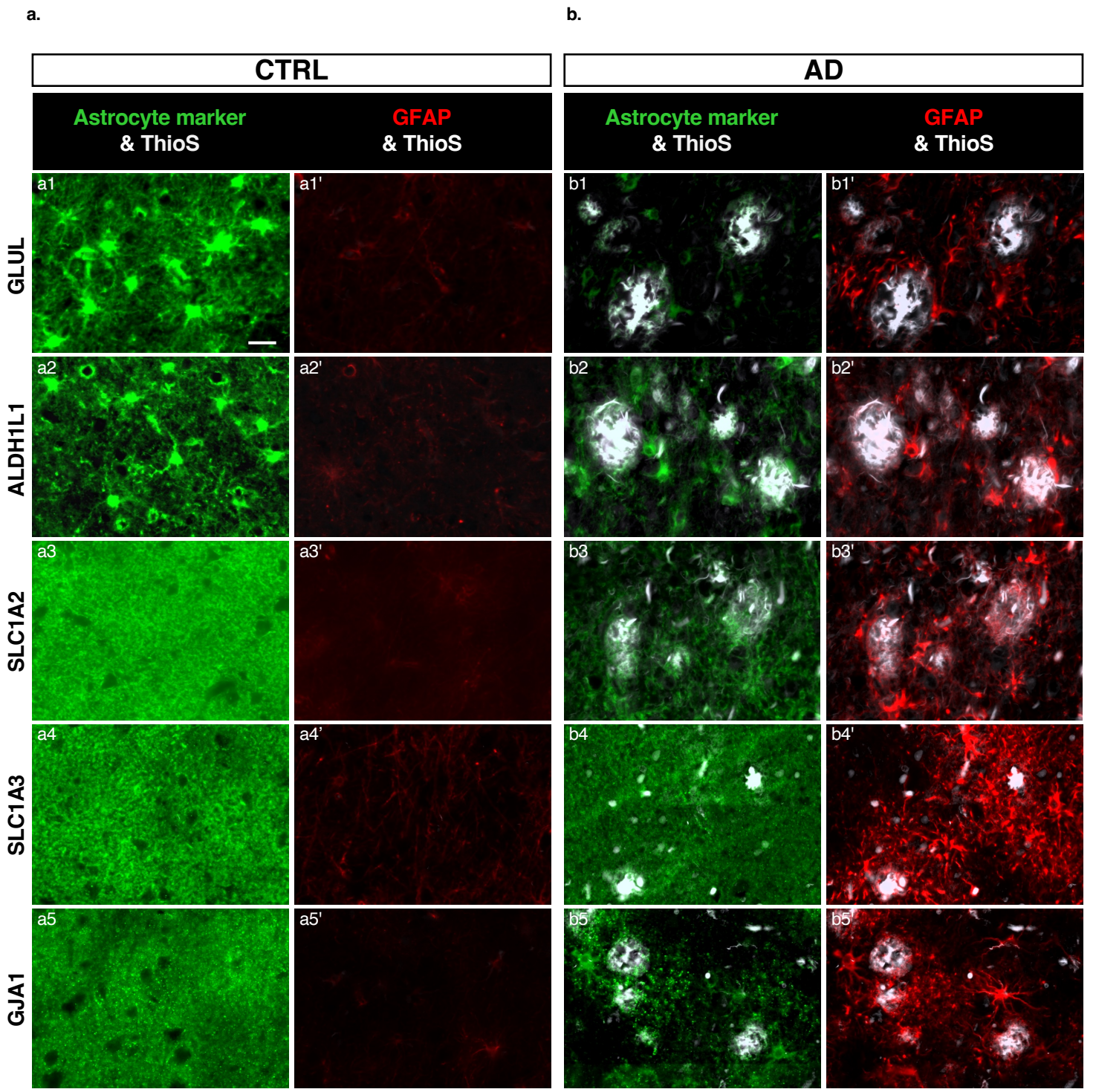
a.
b.
CTRL
AD
Astrocyte marker & ThioS
GFAP & ThioS
Astrocyte marker & ThioS
GFAP & ThioS
GLUL
ALDH1L1
SLC1A2
SLC1A3
GJA1
a1
a1'
b1
b1'
a2
a2'
b2
b2'
a3
a3'
b3
b3'
a4
a4'
b4
b4'
a5
a5'
b5
b5'

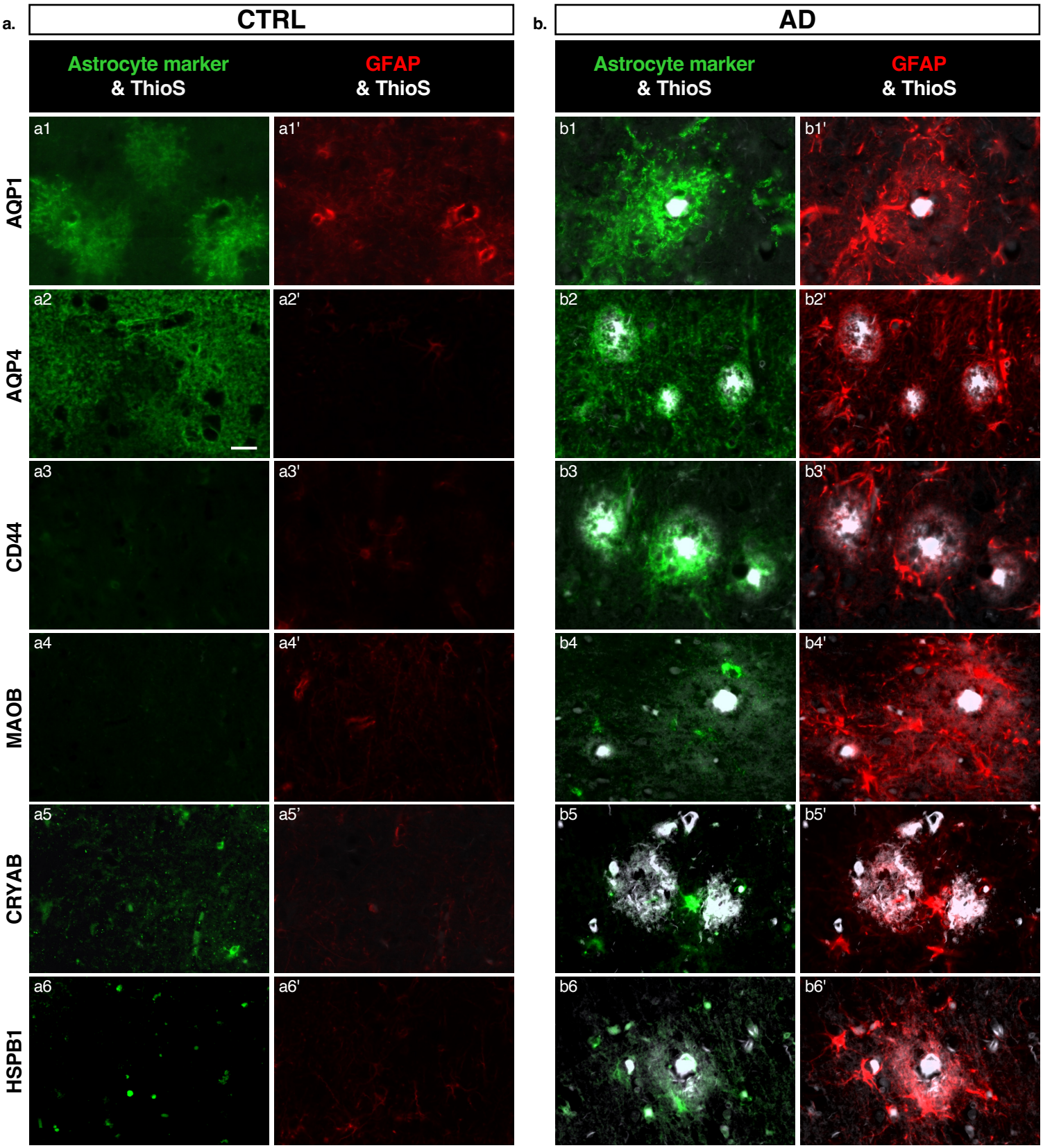
a.
CTRL
b.
AD
Astrocyte marker & ThioS
GFAP & ThioS
Astrocyte marker & ThioS
GFAP & ThioS
AQP1
AQP4
CD44
MAOB
CRYAB
HSPB1
a1
a1'
a2
a2'
a3
a3'
a4
a4'
a5
a5'
a6
a6'
b1
b1'
b2
b2'
b3
b3'
b4
b4'
b5
b5'
b6
b6'

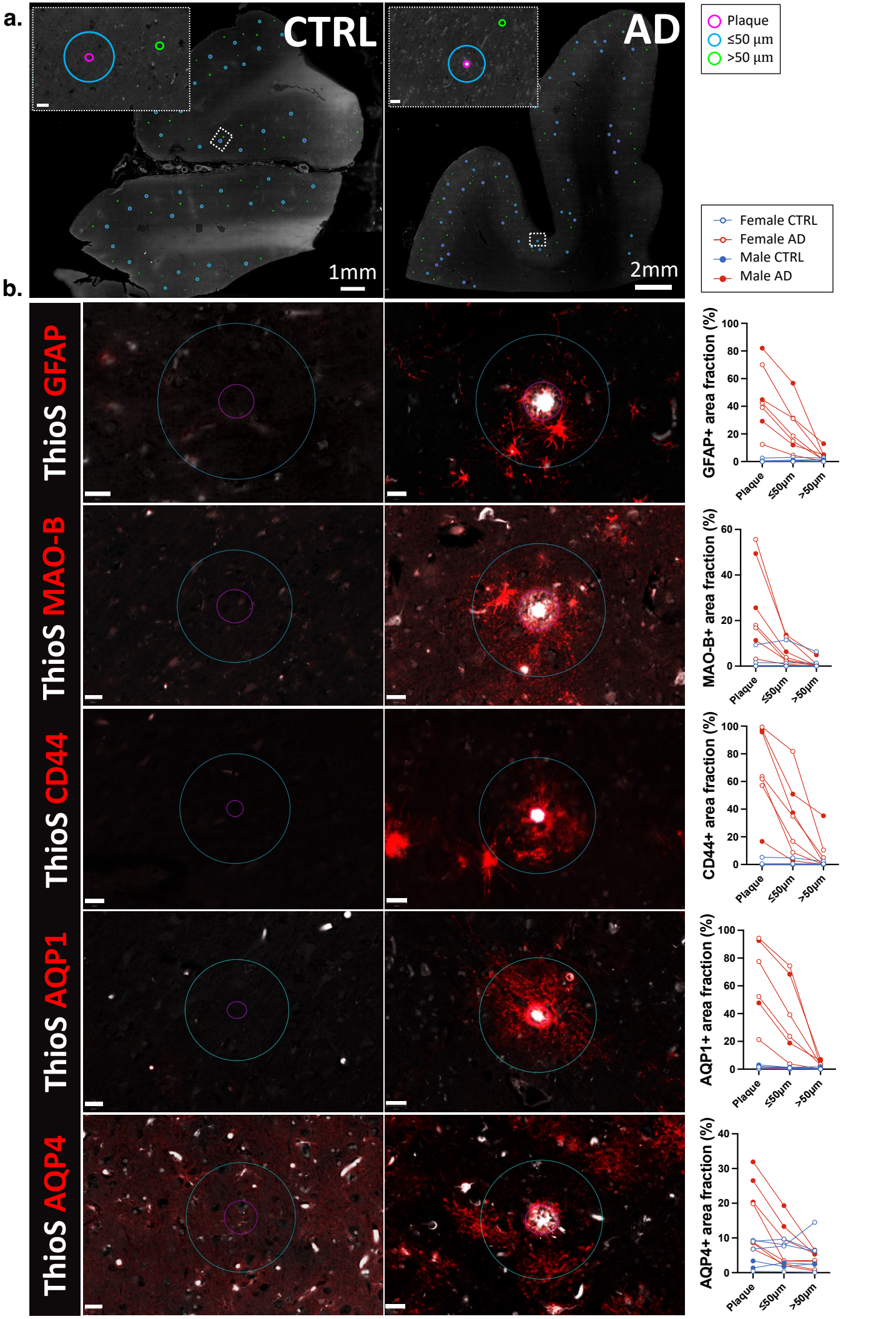
a.
CTRL
AD
Plaque
≤50 µm
>50 µm
1mm
2mm
b.
Female CTRL
Female AD
Male CTRL
Male AD
ThioS GFAP
ThioS MAO-B
ThioS CD44
ThioS AQP1
ThioS AQP4
GFAP+ area fraction (%)
MAO-B+ area fraction (%)
CD44+ area fraction (%)
AQP1+ area fraction (%)
AQP4+ area fraction (%)
Plaque
≤50µm
>50µm

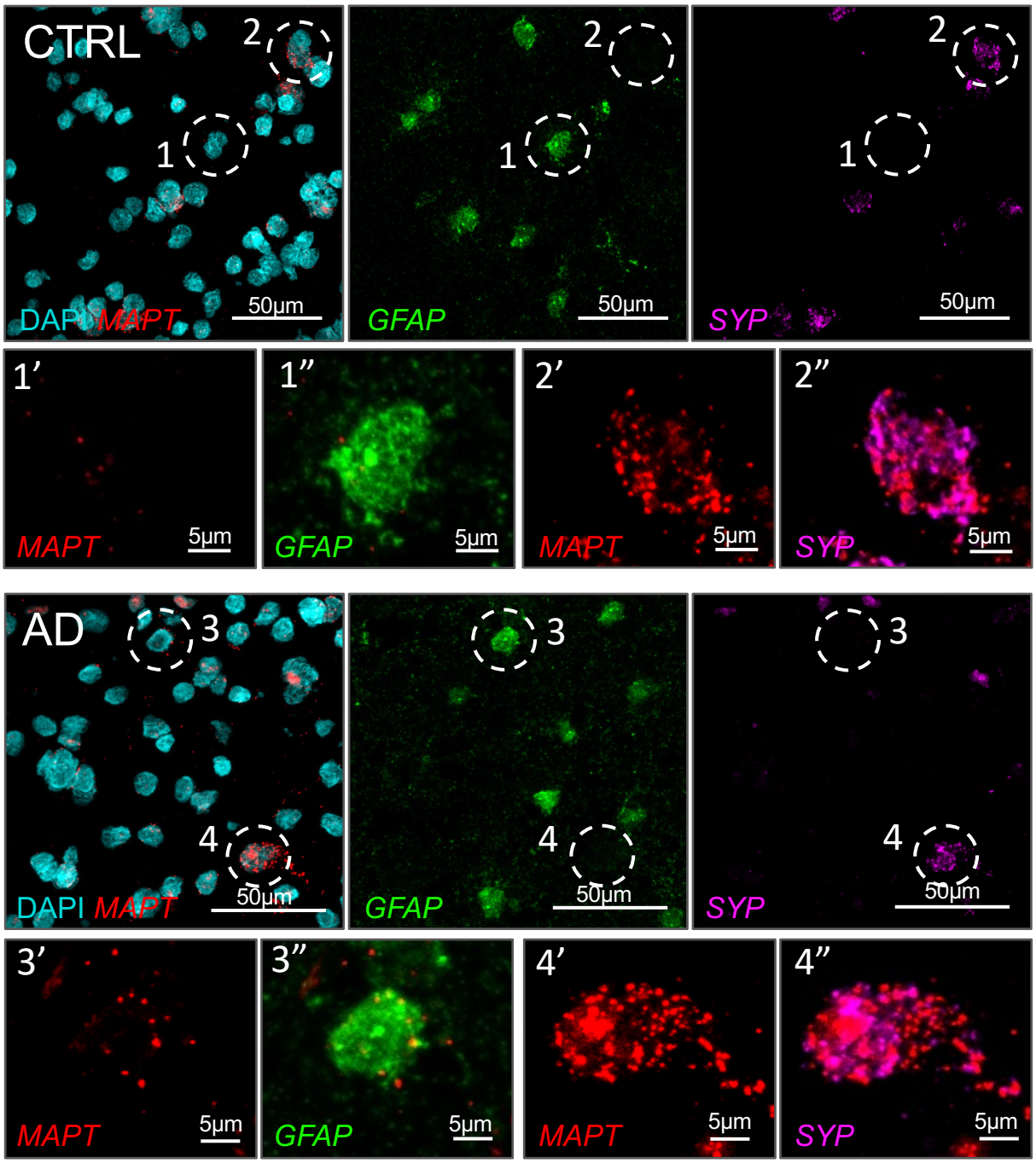
CTRL
2
1
DAPI MAPT
50μm
GFAP
50μm
SYP
50μm
1'
MAPT
5μm
1"
GFAP
5μm
2'
MAPT
5μm
2"
SYP
5μm
AD
3
4
DAPI MAPT
50μm
GFAP
50μm
SYP
50μm
3'
MAPT
5μm
3"
GFAP
5μm
4'
MAPT
5μm
4"
SYP
5μm

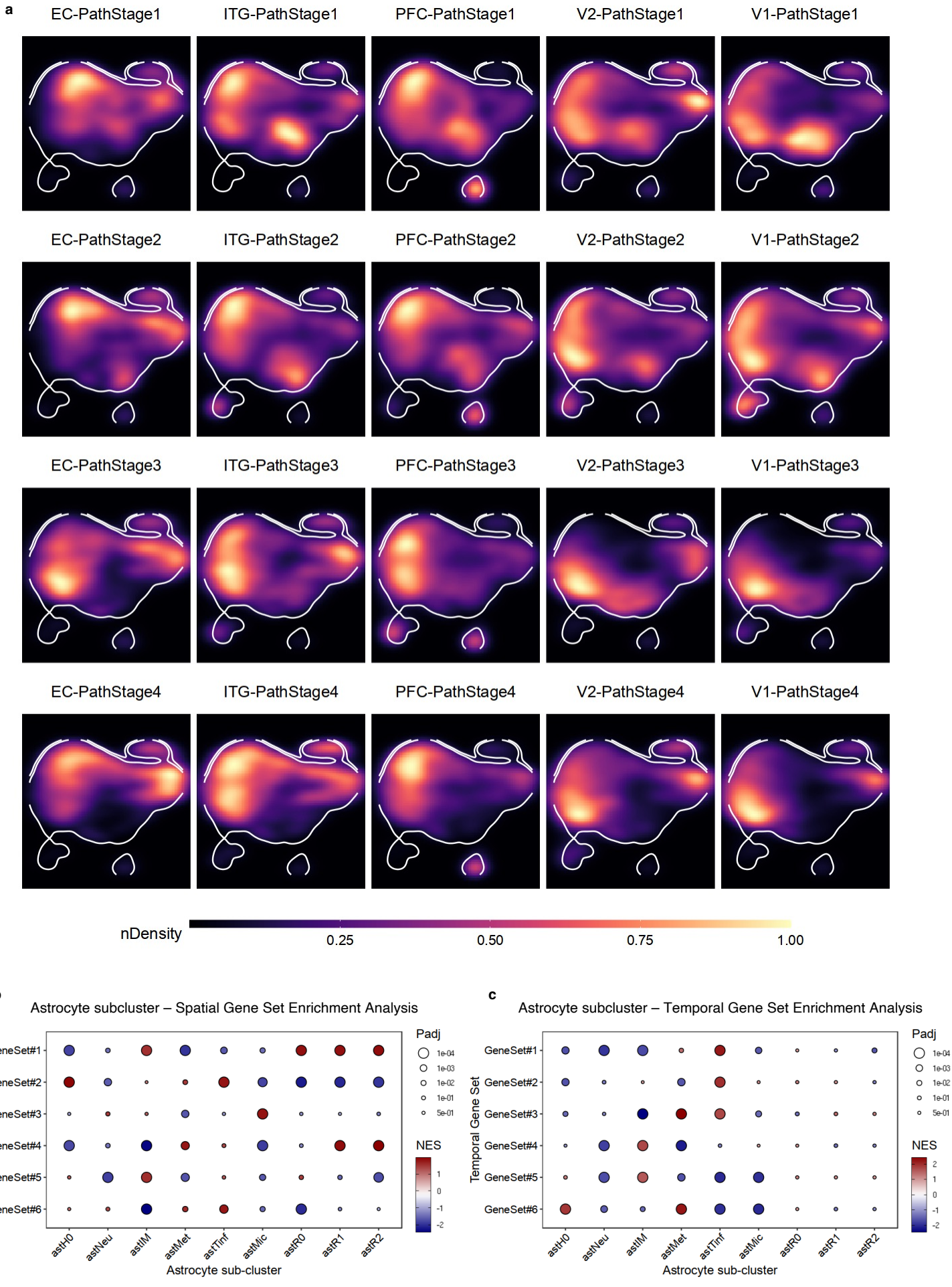
a
EC-PathStage1
ITG-PathStage1
PFC-PathStage1
V2-PathStage1
V1-PathStage1
EC-PathStage2
ITG-PathStage2
PFC-PathStage2
V2-PathStage2
V1-PathStage2
EC-PathStage3
ITG-PathStage3
PFC-PathStage3
V2-PathStage3
V1-PathStage3
EC-PathStage4
ITG-PathStage4
PFC-PathStage4
V2-PathStage4
V1-PathStage4
nDensity
0.25
0.50
0.75
1.00
b
Astrocyte subcluster – Spatial Gene Set Enrichment Analysis
Spatial Gene Set
GeneSet#1
GeneSet#2
GeneSet#3
GeneSet#4
GeneSet#5
GeneSet#6
astH0
astNeu
astIM
astMet
astTnf
astMic
astR0
astR1
astR2
Astrocyte sub-cluster
Padj
1e-04
1e-03
1e-02
1e-01
5e-01
NES
1
0
-1
-2
c
Astrocyte subcluster – Temporal Gene Set Enrichment Analysis
Temporal Gene Set
GeneSet#1
GeneSet#2
GeneSet#3
GeneSet#4
GeneSet#5
GeneSet#6
astH0
astNeu
astIM
astMet
astTnf
astMic
astR0
astR1
astR2
Astrocyte sub-cluster
Padj
1e-04
1e-03
1e-02
1e-01
5e-01
NES
2
1
0
-1
-2

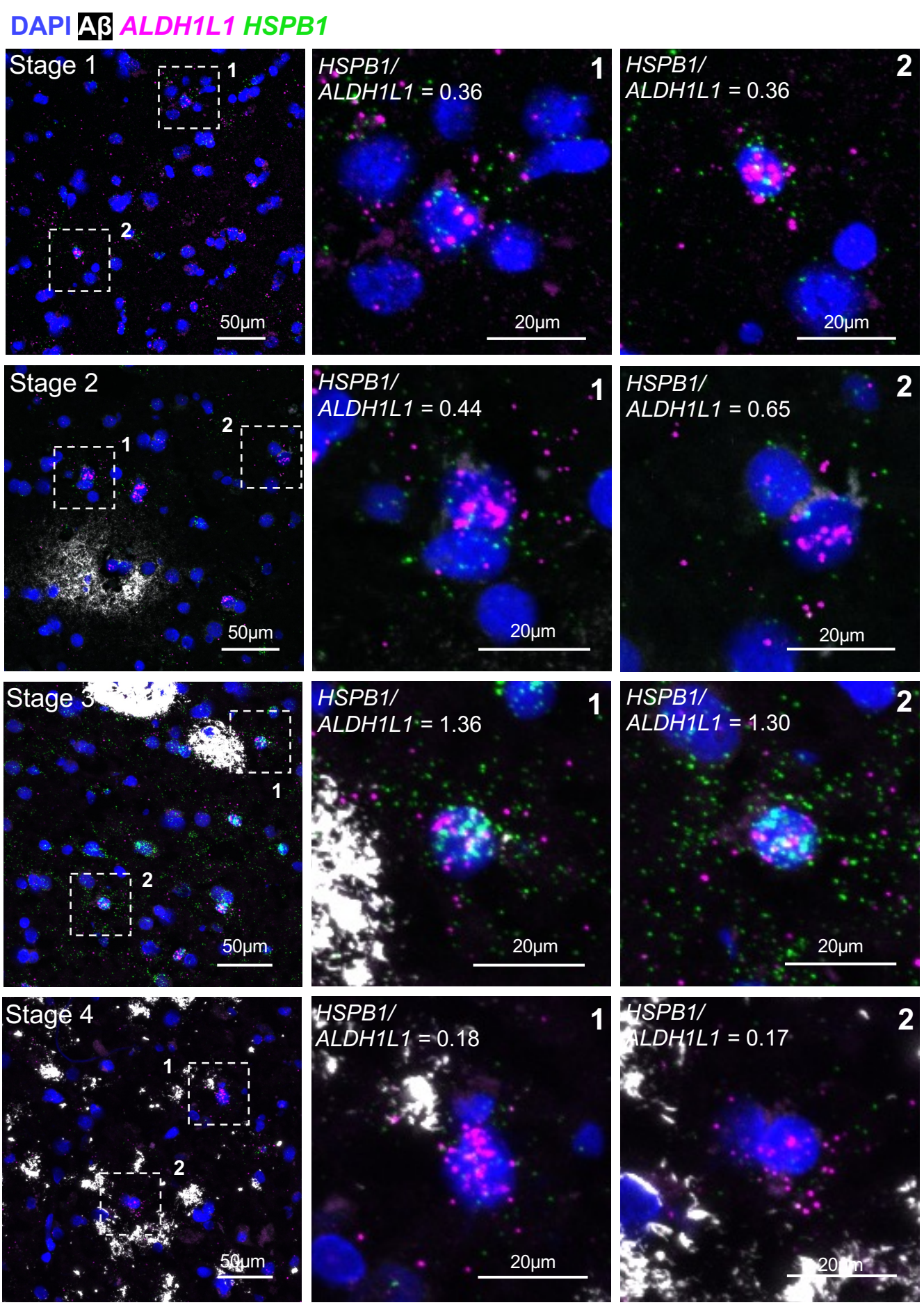
DAPI Aβ ALDH1L1 HSPB1
Stage 1
1
2
50μm
HSPB1/
ALDH1L1 = 0.36
1
20μm
HSPB1/
ALDH1L1 = 0.36
2
20μm
Stage 2
1
2
50μm
HSPB1/
ALDH1L1 = 0.44
1
20μm
HSPB1/
ALDH1L1 = 0.65
2
20μm
Stage 3
1
2
50μm
HSPB1/
ALDH1L1 = 1.36
1
20μm
HSPB1/
ALDH1L1 = 1.30
2
20μm
Stage 4
1
2
50μm
HSPB1/
ALDH1L1 = 0.18
1
20μm
HSPB1/
ALDH1L1 = 0.17
2
20μm

SUPPLEMENTARY FIGURES LEGENDS

Supplementary Figure 1. Characteristics of our snRNA-seq study. a, Example scatterplot of gating strategy for a sample. **b**, Comparison of our AD progression study data with previously published snRNA-seq AD datasets in number of cells, average total number of reads per cell, and average number of detected genes (counts > 0) per cell. **c**, Box plots show the Aβ plaque load (immunoreactive % area fraction) and pTau/Tau ratio (measured by ELISA) of the 32 donors across pathology stages and brain regions. Horizontal line in each box represents the median value; boxes extend from the 25th to the 75th percentile of values in each group; whiskers extend from the 5th to the 95th percentile. Each dot represents one unique sample.

Supplementary Figure 2. Higher aquaporin-4 (AQP4) expression in EC vs. V1 from control donors. Formalin-fixed paraffin-embedded sections from EC and V1 of control donors in Fig. 2c were immunostained for AQP4 with the peroxidase-DAB method in an automated stainer for quantification of AQP4 immunoreactive area fraction. Shown here are of 8 out of 11 control donors in Fig. 2c. Scale bars: 2 mm, insets 500 μm.

Supplementary Figure 3. Higher connexin-43 (GJA1) expression in EC vs. V1 from control donors. Formalin-fixed paraffin-embedded sections from EC and V1 of control donors in Fig. 2c were immunostained for GJA1 with the peroxidase-DAB method in an automated stainer for quantification of GJA1 immunoreactive area fraction. Shown here are of 8 out of 11 control donors in Fig. 2c. Scale bars: 2 mm, insets 500 μm.

Supplementary Figure 4. Spatial and temporal trajectory gene sets expression analysis. a, Left: Heatmap of donor-level expression of spatial trajectory genes (n=512) across 5 regions with logFC. Right: Heatmap of donor-level expression of temporal trajectory genes (n=806) across 4 pathology stages with logFC. **B,** Violin plot of donor-level expression of example genes from spatial trajectory gene sets (S_GS) and temporal trajectory gene sets (T_GS). **c,** Scatter dot plots show the correlation between the average standardized expression of each spatial trajectory gene set in each donor and their Aβ plaque load (top) or pTau/Tau ratio (bottom). Grey shading represents 95% confidence intervals. P-values are determined by linear mixed-effects models. **d,** Venn diagrams show the overlap between each of the spatial trajectory gene sets and the EC- and V1-upregulated (red) and -downregulated (blue) genes. **e,** Overlap of spatial and temporal gene sets.

Supplementary Figure 5. Immunohistochemical analysis of homeostatic astrocyte markers. Double fluorescent immunohistochemistry for GFAP and classic homeostatic astrocyte markers with Thioflavin-S (ThioS) counterstaining in control (**a**) and AD (**b**) formalin-fixed paraffin-embedded sections from the temporal association cortex. Note some reduced expression of these markers in reactive (GFAP+) astrocytes surrounding dense-core (ThioS+) Aβ plaques in AD but an apparent redistribution of GJA1 towards Aβ plaques. Note: Representative photomicrographs from one CTRL and one AD donor taken with similar exposure time and display settings for appropriate comparison (at least 3 CTRL and 3 AD donors were evaluated). Scale bar: 20 μm. CTRL: Control.

Supplementary Figure 6. Immunohistochemical analysis of reactive astrocyte markers. Double fluorescent immunohistochemistry for GFAP and relevant reactive astrocyte markers with Thioflavin-S (ThioS) counterstaining in control (**a**) and AD (**b**) formalin-fixed paraffin-embedded sections from the

temporal association cortex. Note the increased expression of these markers in reactive (GFAP+) astrocytes surrounding dense-core (ThioS+) Aβ plaques and an apparent redistribution of AQP4 toward Aβ plaques in AD. Note: Representative photomicrographs from one CTRL and one AD donor taken with similar exposure time and display settings for appropriate comparison (at least 3 CTRL and 3 AD donors were evaluated). Scale bar: 20 μm. CTRL: Control.

Supplementary Figure 7. Plaque-centered immunohistochemical quantitative analyses. a. Methodology for plaque-centered immunohistochemical analyses. Fifty random Thioflavin-S (ThioS) positive dense-core plaques from n=7 AD (Braak V/VI, 4 females and 3 males) or sham plaques of similar size from n=6 control donors (Braak 0/I/II, 4 females and 2 males) were circled (magenta) and a 50 μm halo (blue) was generated; in addition, fifty circular regions of interest located >50 μm from the nearest plaque edge (green) were also overlaid on the images. Scale bars: CTRL, 1 mm; AD, 2 mm; insets, 20 μm. **b.** Quantification of selected astrocyte reactive markers in ThioS+ Aβ plaques or sham plaques, their vicinity (≤50 μm), and distant areas (>50 μm). Data and statistics are shown in Fig. 5e. Here, connecting lines identify the same donor across the three locations with each symbol representing the immunoreactive area fraction (%) within all 50 annotations of each location for each donor. Scale bars: 20 μm. Note: pseudocolored white fluorescent signal in some control donors is autofluorescence from capillaries.

Supplementary Figure 8. *In situ* hybridization (RNAScope) analysis of *MAPT*. RNAScope for *MAPT*, *GFAP*, and *SYP* (encoding the neuronal synaptic marker synapsin) reveals some expression of *MAPT* in astrocytes. Cells 1 and 3 are astrocytes (*GFAP*+ve), whereas cells 2 and 4 are neurons (*SYP*+ve). Note: Representative photomicrographs from one CTRL and one AD donor taken with

similar exposure time and display settings for appropriate comparison (at least 3 CTRL and 3 AD donors were evaluated).

Supplementary Figure 9. Subcluster characterization along spatial and temporal axes. a, Subcluster density along spatial and temporal progression. **b**, Enrichment of spatial gene sets in subcluster marker genes. **c,** Enrichment of temporal gene sets in subcluster marker genes. Homeostatic and reactive markers were enriched in spatial gene sets that were correlated to pTau/Tau and the temporal gene sets were enriched in the intermediate subcluster marker genes. NES stands for normalized enrichment score determined by gene set enrichment analysis.

Supplementary Figure 10. *In situ* hybridization of astrocytic *HSPB1* across pathology stages. Using *ALDH1L1* as a marker of astrocytes and to control for RNA integrity, representative images show more astrocytic *HSPB1* transcripts in pathology stage 3, compared to stages 1 and 2, which appeared to be distributed throughout cell nuclei and into surrounding processes. Similar to our snRNA-seq results, the number of astrocytic *HSPB1* transcripts increased in pathology stage 3, compared to stages 1 and 2, and subsequently declined in pathology stage 4. Note: Representative photomicrographs from one donor at each pathology stage (3 donors were evaluated at each pathology stage).